Study Of Isotropic Non-Homogeneous Rectangular Plate With Non-Uniform Circularly Varying Thickness And Parabolically Varying Temperature Effect

Umesh Bhardwaj¹, Ashish Kumar Sharma^{1*}

¹Research Scholar, Department of Mathematics, Arni University, Kathgarh, Indora, H.P. India.

^{1*}Department of Mathematics, Arni University, Kathgarh, Indora, H.P. India E-mail: umesh2831993@gmail.com, ashishk482@gmail.com

Rectangular visco-elastic plates are commonly used in many industries, aviation, and mechanical structures. Accurately determining the behaviour and strength properties of plates is necessary for the right design of plate structures and the effective use of material. The frequency of free vibrations of a rectangular visco-elastic plate with varying thickness is examined in relation to two-dimensional thermal effects. In this article, the thermal effect varies parabolically in two directions while the thickness varies circularly in the x-direction. The fundamental frequencies are evaluated using the Rayleigh Ritz method. MATLAB is used to calculate first two modes of frequencies over various values of temperature gradient, non-homogeneity, and taper parameter values.

Key Words:- Vibration, parabolically, circularly, non-homogeneity, isotropic, aspect ratio, taper parameter, thermal gradient, flexural rigidity, strain energy, kinetic energy.

Introduction

Engineers and researchers must always be aware of the system's vibration characteristics when building machines, structures, and other mechanical designs. It is impossible to overlook the significance of researching the vibrations of non-homogeneous tapered plates, which are frequently utilized in the building of bridges, ships, airplanes, and other structures. The material is stronger and lighter due to non-homogeneity and plate tapering. By creating appropriate and precise machine and building designs, the primary goal of vibration research is to prevent unnecessary and excessive vibration. The majority of engineering structures in the current technological period, including nuclear reactors, rockets, and missiles, work with adequate temperature fields under various boundary conditions. Hence, it becomes essential to investigate how temperature changes affect the structures vibrational characteristics. Vibration research primary goal is to minimize unnecessary and excessive vibration by accurately and appropriately constructing mechanical structures.

Studied the effect of bi-parabolic temperature variation on the vibration of an orthotropic rectangular plate, highlighting the importance of thermal sensitivity in structural analysis [1]. A simple model analyses the thermal effect on the vibration of a non-homogeneous orthotropic visco-elastic rectangular plate with parabolically varying thickness and clamped edges, using the Rayleigh-Ritz technique to derive an approximate frequency equation[2]. This paper presents a unified nonlinear analytical solution for bending, buckling, and vibration of temperature-dependent functionally graded rectangular plates under thermal load, comparing three mathematical models for effective material properties [3]. The study analyses the vibration frequencies of a rectangular plate with a linearly varying thickness and a circularly varying Poisson's ratio[4]. The paper presents a mathematical model to analyse the temperature-thickness coupling in a non-homogeneous isotropic viscoelastic rectangular plate with bi-parabolic temperature variation, linear thickness variation, and exponential Poisson's ratio variation[5]. The paper analyses the buckling loads of rectangular composite plates under non-uniform in-plane loading using higher-order shear deformation theory, solving for stress distribution and buckling equations to obtain critical loads and mode shapes[6]. The paper investigates the buckling behaviour of symmetrically laminated rectangular plates under parabolic in-plane compressive loading using the Rayleigh-Ritz method, incorporating Chebyshev polynomials to derive buckling loads for various boundary conditions and validating results against DQM and FEM[7]. The paper analyses the vibrational frequencies of a non-homogeneous viscoelastic parallelogram plate with circular thickness variation and biparabolic temperature distribution using the Rayleigh-Ritz method and MAPLE software[8]. The paper presents a nonlinear vibration analysis of functionally graded rectangular microplates with variable thickness and a central partial crack using Classical Plate Theory and modified couple stress theory, demonstrating how thickness variation can mitigate crack effects on vibration characteristics[9]. The effect of two-parameter foundation on the transverse vibrations and critical buckling loads of nonhomogeneous rectangular plates under linearly varying in-plane forces has been analysed using the Kirchhoff plate theory and solved numerically via the Levy approach and Differential Quadrature Method[10]. The natural transverse vibration of a nonhomogeneous skew plate with variable thickness and temperature field is analysed using the Rayleigh-Ritz technique under CCCC and CSCS edge conditions[11]. Free transverse vibrations of isotropic rectangular plates with arbitrarily varying non-homogeneity are analysed using the Generalized Differential Quadrature Method based on Kirchhoff plate theory[12]. The Rayleigh-Ritz method is used to analyse the natural vibration time period of an isotropic viscoelastic square plate with circular thickness variation and Poisson's ratio under clamped and simply supported conditions[13]. This paper investigates the natural vibration of a non-uniform, non-homogeneous square plate with clamped boundaries, considering circular thickness variation, bi-linear temperature distribution, and linear density variation using the Rayleigh-Ritz method[14]. This paper analyzes the natural vibration of a non-uniform, non-homogeneous square plate with clamped boundaries, considering thickness variation, bi-linear temperature distribution, and density variation using the Rayleigh-Ritz method[15]. The vibration of a tapered isotropic rectangular plate under thermal conditions is analyzed using the Rayleigh-Ritz method for various boundary conditions[16]. The effect of linear thickness variation on the vibration of a viscoelastic rectangular plate with clamped edges is analyzed using the Rayleigh-Ritz

method[17]. The Rayleigh Ritz method is used to solve the differential equation involving the linear density variation and the circular Poisson's ratio fluctuation on the vibration time period of the rectangular plate[18]. A tapered, non-homogeneous rectangular plate with a variety of boundary conditions is used to examine plate properties[19]. The effect of bilinear temperature variation on the vibration of a non-homogeneous viscoelastic rectangular plate with non-uniform thickness is analyzed using the Rayleigh–Ritz method[20].

In addition to using aspect ratios of 1.5 and 2.5, the deflection function is utilized to identify the modes of frequency for various values of temperature gradient, taper constant, and non-homogeneity. With SSSS boundary conditions and a two-dimensional temperature field distribution, the Rayleigh-Ritz technique is used to study the natural vibration of an isotropic non-homogeneous rectangular plate with a one-dimensional circularly variable thickness and density parameter.

A rectangular plate composed of duralumin material with a circular variation in thickness in one direction was used to achieve the solution of the first two modes of vibration in the current experiment. Both tabular and graph formats are used to display the numerical values of the first two modes of the frequency at different structural parameter values for the SSSS boundary condition, assuming that the plate is simply supported on all four edges.

Analysis Of Equation Of Motion

The differential equation of motion of visco-elastic isotropic plate may be written as [16]

$$\frac{\partial^2 \tau_x}{\partial x^2} + 2 \frac{\partial^2 \tau_{xy}}{\partial x \partial y} + \frac{\partial^2 \tau_y}{\partial y^2} = \rho h \frac{\partial^2 \xi}{\partial t^2}$$

(1)

where x and y represent the plate geometry's coordinates, τ_x and τ_y represent the bending moments, τ_{xy} represents the twisting moment per unit plate length, ρ represents the mass per unit volume, h represents the plate's thickness, and ξ represents the displacement at time t.

The expressions for τ_x , τ_v and τ_{xv} are given by [17]

$$\begin{split} \tau_{x} &= -\tilde{D}D_{1}\left[\frac{\partial^{2}\xi}{\partial x^{2}} + \nu \frac{\partial^{2}\xi}{\partial y^{2}}\right], \\ \tau_{y} &= -\tilde{D}D_{1}\left[\frac{\partial^{2}\xi}{\partial x^{2}} + \nu \frac{\partial^{2}\xi}{\partial y^{2}}\right] \text{ and } \\ \tau_{xy} &= -\tilde{D}D_{1}(1 - \nu) \frac{\partial^{2}\xi}{\partial x \partial y} \end{split}$$

(2)

where \tilde{D} is the representation for visco-elastic operator. In this case, D_1 represents the material's flexural rigidity and is written as[18]

$$D_1 = \frac{Eh^3}{12(1-v^2)}$$

(3)

When τ_x , τ_y and τ_{xy} are substituted in equation (1), one obtains

$$\begin{split} \widetilde{D}\left[D_{1}\left(\frac{\partial^{4}\xi}{\partial x^{4}}+2\frac{\partial^{4}\xi}{\partial x^{2}\frac{\partial y^{2}}{\partial y^{2}}+\frac{\partial^{4}\xi}{\partial y^{4}}\right)+2\frac{\partial D_{1}}{\partial x}\left(\frac{\partial^{3}\xi}{\partial x^{3}}+2\frac{\partial^{3}\xi}{\partial x\partial y^{2}}\right)+2\frac{\partial D_{1}}{\partial y}\left(\frac{\partial^{3}\xi}{\partial y^{3}}+2\frac{\partial^{3}\xi}{\partial y\partial x^{2}}\right)\\ +\frac{\partial^{2}D_{1}}{\partial x^{2}}\left(\frac{\partial^{2}\xi}{\partial x^{2}}+\nu\frac{\partial^{2}\xi}{\partial y^{2}}\right)+\frac{\partial^{2}D_{1}}{\partial y^{2}}\left(\frac{\partial^{2}\xi}{\partial y^{2}}+\nu\frac{\partial^{2}\xi}{\partial x^{2}}\right)+2(1-\nu)\frac{\partial^{2}D_{1}}{\partial x\partial y}\frac{\partial^{2}\xi}{\partial x\partial y}\right]+\rho h\frac{\partial^{2}\xi}{\partial t^{2}}=0 \end{split} \tag{4}$$

Deflection ξ can be considered the product of two functions using the variable separation method[19] $\xi(x,y,t) = \varphi(x,y) \cdot T(t)$ (5)

where T(t) is a time function for the vibration of a rectangular plate and $\phi(x, y)$ is the deflection function in x and y. Equation (5) can be substituted into equation (4), to get

$$\begin{split} \left[D_{1} \left(\frac{\partial^{4} \varphi}{\partial x^{4}} + 2 \frac{\partial^{4} \varphi}{\partial x^{2}} \frac{\partial^{4} \varphi}{\partial y^{2}} + \frac{\partial^{4} \varphi}{\partial y^{4}} \right) + 2 \frac{\partial D_{1}}{\partial x} \left(\frac{\partial^{3} \varphi}{\partial x^{3}} + 2 \frac{\partial^{3} \varphi}{\partial x \partial y^{2}} \right) + 2 \frac{\partial D_{1}}{\partial y} \left(\frac{\partial^{3} \varphi}{\partial y^{3}} + 2 \frac{\partial^{3} \varphi}{\partial y \partial x^{2}} \right) \\ + \frac{\partial^{2} D_{1}}{\partial x^{2}} \left(\frac{\partial^{2} \varphi}{\partial x^{2}} + \nu \frac{\partial^{2} \varphi}{\partial y^{2}} \right) + \frac{\partial^{2} D_{1}}{\partial y^{2}} \left(\frac{\partial^{2} \varphi}{\partial y^{2}} + \nu \frac{\partial^{2} \varphi}{\partial x^{2}} \right) + 2 (1 - \nu) \frac{\partial^{2} D_{1}}{\partial x \partial y} \frac{\partial^{2} \varphi}{\partial x \partial y} \right] / \rho h \varphi = - \left(\frac{\partial^{2} T / \partial t^{2}}{\tilde{D} T} \right) \end{split}$$

$$(6)$$

When both sides of equation (6) are equal to a constant p^2 , the result is

$$\begin{split} \left[D_1 \left(\frac{\partial^4 \varphi}{\partial x^4} + 2 \frac{\partial^4 \varphi}{\partial x^2 \partial y^2} + \frac{\partial^4 \varphi}{\partial y^4} \right) + 2 \frac{\partial D_1}{\partial x} \left(\frac{\partial^3 \varphi}{\partial x^3} + 2 \frac{\partial^3 \varphi}{\partial x \partial y^2} \right) + 2 \frac{\partial D_1}{\partial y} \left(\frac{\partial^3 \varphi}{\partial y^3} + 2 \frac{\partial^3 \varphi}{\partial y \partial x^2} \right) \\ + \frac{\partial^2 D_1}{\partial x^2} \left(\frac{\partial^2 \varphi}{\partial x^2} + \nu \frac{\partial^2 \varphi}{\partial y^2} \right) + \frac{\partial^2 D_1}{\partial y^2} \left(\frac{\partial^2 \varphi}{\partial y^2} + \nu \frac{\partial^2 \varphi}{\partial x^2} \right) + 2 (1 - \nu) \frac{\partial^2 D_1}{\partial x \partial y} \frac{\partial^2 \varphi}{\partial x \partial y} \right] - \rho p^2 h \varphi &= 0 \end{split}$$

$$(7)$$

and

$$\frac{\partial^2 T}{\partial t^2} + p^2 \tilde{D}T = 0$$
(8)

Assumption Required

one dimensional circular variation in thickness as [18]

$$h = h_0 \left[1 + \beta \left(1 - \sqrt{1 - \frac{x^2}{a^2}} \right) \right]$$

(9)

where β , $(0 \le \beta \le 1)$ is known as tapering parameter and thickness of plate becomes constant at x = 0 and for non-homogeneity (ρ) consideration, assumed one dimensional circular variation in Poisson's ratio as

$$\rho = \rho_0 \left[1 + m_2 \frac{x}{a} \right], \tag{10}$$

$$\nu = \nu_0 \left[1 - m_1 \left(1 - \sqrt{1 - \frac{x^2}{a^2}} \right) \right]$$
 (11)

where m_2 , $(0 \le m_2 \le 1)$ and m_1 $(0 \le m_1 < 1)$ are known as non-homogeneity constant corresponding to density and Poisson's ratio.

The plate is subjected to steady two-dimensional parabolically varying temperature distributions as[11]

$$\bar{\tau} = \bar{\tau_0} \left(1 - \frac{x^2}{a^2} \right) \left(1 - \frac{y^2}{a^2} \right)$$
(12)

Therefore the temperature dependent modulus of elasticity is taken as [16]

(13)
$$E(\tau) = E_0(1-\gamma \overline{\tau}_0)$$

$$E(\tau) = E_0\left[1-\gamma \overline{\tau}_0\left(1-\frac{x^2}{a^2}\right)\left(1-\frac{y^2}{a^2}\right)\right]$$

$$E(\tau) = E_0\left[1-\alpha\left(1-\frac{x^2}{a^2}\right)\left(1-\frac{y^2}{a^2}\right)\right]$$
(14)

Where $\alpha = \gamma \overline{\tau_0}$, $(0 \le \alpha < 1)$

Boundary Condition

For SSSS, the boundary conditions are [19]

$$\phi = \frac{\partial^2 \phi}{\partial x^2} = 0$$
 at $x = 0$, a and $\phi = \frac{\partial^2 \phi}{\partial y^2} = 0$ at $y = 0$, b

The deflection function (i.e. maximum displacement) which satisfy boundary condition given in as:

$$\varphi\left(x,y\right) = \left(\frac{x}{a}\right)\left(\frac{y}{b}\right)\left(1 - \frac{x}{a}\right)\left(1 - \frac{y}{b}\right)\left[A_1 + A_2\left(\frac{x}{a}\right)\left(\frac{y}{b}\right)\left(1 - \frac{x}{a}\right)\left(1 - \frac{y}{b}\right)\right]$$
(15)

where A_1 and A_2 are arbitrary constants.

Rayleigh Ritz Method In Rectangular Plate

We are using Rayleigh Ritz technique (i.e., maximum strain energy S_E must equal to maximum kinetic energy K_E) in order to obtain frequency equation for both modes of vibrations. As a result, we need to have:

$$\delta(S_E - K_E) = 0$$

(16)

The K_E and S_E formula are provided by [20]

$$K_E = \frac{1}{2} P^2 \int_0^a \int_0^b \rho h \phi^2 dx dy$$
 (17)

$$S_{E} = \frac{1}{2} \int_{0}^{a} \int_{0}^{b} D_{1} \times \left[\left(\frac{\partial^{2} \phi}{\partial x^{2}} \right)^{2} + \left(\frac{\partial^{2} \phi}{\partial y^{2}} \right)^{2} + 2\nu \frac{\partial^{2} \phi}{\partial x^{2}} \frac{\partial^{2} \phi}{\partial y^{2}} + 2(1 - \nu) \left(\frac{\partial^{2} \phi}{\partial x \partial y} \right)^{2} \right] dx dy$$
(18)

The non-dimensional variables are outlined to make the computation simple and convenient:

$$X = \frac{x}{a}, Y = \frac{y}{b}, \bar{h} = \frac{h}{a} and \bar{\phi} = \frac{\phi}{a}$$
(19)

Solution Of Frequency Equation

on using the above assumptions along with (19); equation (17) and (18) becomes

$$K_{E} = \frac{1}{2}p^{2} \int_{0}^{a} \int_{0}^{b} \rho_{0} \left[1 + m_{2} \frac{x}{a} \right] h_{0} \left[1 + \beta \left(1 - \sqrt{1 - \frac{x^{2}}{a^{2}}} \right) \right] \phi^{2} dy dx$$

$$= \frac{1}{2} \rho_{0} p^{2} h_{0} \int_{0}^{a} \int_{0}^{b} \left[1 + m_{2} \frac{x}{a} \right] \left[1 + \beta \left(1 - \sqrt{1 - \frac{x^{2}}{a^{2}}} \right) \right] \phi^{2} dy dx$$

$$\text{Substituting } X = \frac{x}{a} \qquad \qquad Y = \frac{y}{a}$$

$$x \to 0 \Rightarrow X \to 0 \qquad \qquad y \to 0 \Rightarrow Y \to 0$$

$$x \to a \Rightarrow X \to 1 \qquad \qquad y \to b \Rightarrow Y \to \frac{b}{a}$$

$$K_{E} = \frac{1}{2} \rho_{0} p^{2} h_{0} \int_{0}^{1} \int_{0}^{b/a} \left[1 + m_{2} X \right] \left[1 + \beta \left(1 - \sqrt{1 - X^{2}} \right) \right] \left(\frac{\phi}{a} \right)^{2} a^{2} dX dY$$

$$= \frac{1}{2} \rho_{0} p^{2} h_{0} \int_{0}^{1} \int_{0}^{b/a} \left[1 + m_{2} X \right] \left[1 + \beta \left(1 - \sqrt{1 - X^{2}} \right) \right] \bar{\phi}^{2} a^{4} dX dY$$

$$= \frac{1}{2} \rho_0 P^2 \frac{h_0}{a} a \times a^4 \int_0^1 \int_0^{b/a} [1 + m_2 X] \left[1 + \beta \left(1 - \sqrt{1 - X^2} \right) \right] \bar{\phi}^2 dX dY$$

$$= \frac{1}{2} p_0 p^2 \overline{h_0} a^5 \int_0^1 \int_0^{b/a} [1 + m_2 X] \left[1 + \beta \left(1 - \sqrt{1 - X^2} \right) \right] \bar{\phi}^2 dX dY$$
(20)

And

$$\begin{split} S_E &= \frac{1}{2} \int_0^a \int_0^b D_1 \left[\left(\frac{\partial^2 \phi}{\partial x^2} \right)^2 + \left(\frac{\partial^2 \phi}{\partial y^2} \right)^2 + 2v \frac{\partial^2 \phi}{\partial x^2} \frac{\partial^2 \phi}{\partial y^2} + 2(1-v) \left(\frac{\partial^2 \phi}{\partial x \partial y} \right)^2 \right] dx dy \\ &= \frac{1}{2} \int_0^a \int_0^b \frac{Eh^3}{12(1-v^2)} \left[\left(\frac{\partial^2 \phi}{\partial x^2} \right)^2 + \left(\frac{\partial^2 \phi}{\partial y^2} \right)^2 + 2v \frac{\partial^2 \phi}{\partial x^2} \frac{\partial^2 \phi}{\partial y^2} + 2(1-v) \left(\frac{\partial^2 \phi}{\partial x \partial y} \right)^2 \right] dx dy \\ &= \frac{1}{24(1-v^2)} \int_0^a \int_0^b E_0 \left[1 - \alpha \left(1 - \frac{x^2}{a^2} \right) \left(1 - \frac{y^2}{a^2} \right) \right] h_0^3 \left[1 + \beta \left(1 - \frac{x^2}{a^2} \right) \right]^3 \left[\left(\frac{\partial^2 \phi}{\partial x^2} \right)^2 + \left(\frac{\partial^2 \phi}{\partial y^2} \right)^2 + \left(\frac{\partial^2 \phi}{\partial y^2} \right)^2 + 2(1-v) \left(\frac{\partial^2 \phi}{\partial x^2} \right)^2 \right] dx dy \\ &= \frac{E_0 h_0^3}{a^2} \left[\left(1 - \frac{x^2}{a^2} \right) \right] \left[1 + \beta \left(1 - \sqrt{1 - \frac{x^2}{a^2}} \right) \right]^3 \left[\left(\frac{\partial^2 \phi}{\partial x^2} \right)^2 + \left(\frac{\partial^2 \phi}{\partial y^2} \right)^2 + 2(1-v) \left(\frac{\partial^2 \phi}{\partial x^2} \right)^2 \right] dx dy \\ &= \frac{Eh_0^3 a^3}{24(1-v^2)} \int_0^1 \int_0^{b/a} \left[1 - \alpha (1-X^2)(1-Y^2(a/b)) \left[1 + \beta \left(1 - \sqrt{1-X^2} \right) \right]^3 \left[\left(\frac{\partial^2 \phi}{\partial x^2} \right)^2 + 2(1-v) \left(\frac{\partial^2 \phi}{\partial x^2} \right)^2 \right] dx dy \\ &= \frac{Eh_0^3 a^3}{24(1-v^2)} \int_0^1 \int_0^{b/a} \left[1 - \alpha (1-X^2)(1-Y^2(a/b)) \left[1 + \beta \left(1 - \sqrt{1-X^2} \right) \right]^3 \left[\left(\frac{\partial^2 \phi}{\partial x^2} \right)^2 + 2(1-v) \left(\frac{\partial^2 \phi}{\partial x^2} \right)^2 \right] dx dy \\ &= \frac{Eh_0^3 a^3}{24(1-v^2)} \int_0^1 \int_0^{b/a} \left[1 - \alpha (1-X^2)(1-Y^2(a/b)) \left[1 + \beta \left(1 - \sqrt{1-X^2} \right) \right]^3 \left[\left(\frac{\partial^2 \phi}{\partial x^2} \right)^2 + 2(1-v) \left(\frac{\partial^2 \phi}{\partial x^2} \right)^2 \right] dx dy \\ &= \frac{Eh_0^3 a^3}{24(1-v^2)} \int_0^1 \int_0^{b/a} \left[1 - \alpha (1-X^2)(1-Y^2(a/b)) \left[1 + \beta \left(1 - \sqrt{1-X^2} \right) \right]^3 \left[\left(\frac{\partial^2 \phi}{\partial x^2} \right)^2 + 2(1-v) \left(\frac{\partial^2 \phi}{\partial x^2} \right)^2 \right] dx dy \\ &= \frac{Eh_0^3 a^3}{24(1-v^2)} \int_0^1 \int_0^{b/a} \left[1 - \alpha (1-X^2)(1-Y^2(a/b)) \left[1 + \beta \left(1 - \sqrt{1-X^2} \right) \right]^3 \left[\left(\frac{\partial^2 \phi}{\partial x^2} \right)^2 + 2(1-v) \left(\frac{\partial^2 \phi}{\partial x^2} \right)^2 \right] dx dy \\ &= \frac{2h_0^3 a^3}{24(1-v^2)} \int_0^1 \int_0^{b/a} \left[1 - \alpha (1-X^2)(1-Y^2(a/b)) \left[1 + \beta \left(1 - \sqrt{1-X^2} \right) \right] dx dy dx dy \\ &= \frac{2h_0^3 a^3}{24(1-v^2)} \int_0^1 \int_0^{b/a} \left[1 - \alpha (1-X^2)(1-Y^2(a/b)) \left[1 + \beta \left(1 - \sqrt{1-X^2} \right) \right] dx dy d$$

Using equation (19) and (20) in equation (16) represents the necessary frequency parameter.

$$\delta(S_E^* - \lambda^2 K_E^*) = 0$$
(22)

$$\begin{split} S_E^* &= \int_0^1 \int_0^{b/a} \left[1 - \alpha (1 - X^2) (1 - Y^2(a/b))\right] \left[1 + \beta \left(1 - \sqrt{1 - X^2}\right]^3 \left(\frac{\partial^2 \bar{\phi}}{\partial x^2}\right)^2 + \left(\frac{\partial^2 \bar{\phi}}{\partial y^2}\right)^2 + \\ &+ 2 \nu \frac{\partial^2 \bar{\phi}}{\partial x^2} \frac{\partial^2 \bar{\phi}}{\partial y^2} + 2 (1 - \sqrt{1 - X^2})^2 \right] + \frac{\partial^2 \bar{\phi}}{\partial x^2} \left(\frac{\partial^2 \bar{\phi}}{\partial y^2}\right)^2 + \frac{\partial^2 \bar{\phi}}{\partial y^2} \left(\frac{\partial^2 \bar{\phi$$

$$\nu) \left(\frac{\partial^2 \bar{\phi}}{\partial x \partial y} \right)^2 dX dY \tag{23}$$

$$k_E^* = \int_0^1 \int_0^{b/a} [1 + m_2 X] [1 + \beta (1 - \sqrt{1 - X^2})] \bar{\phi}^2 dX dY$$
(24)

Here expression of the required frequency parameter is

$$\lambda^2 = \frac{12\rho_0 p^2 a^2 (1 - \nu^2)}{E_0 \bar{h}_0^2}$$
(25)

Equation (22) contains two unknown constants, A_1 and A_2 which result from the substitution of deflection function $\phi(x, y)$.

The following formula could be used to determine these two unknowns:

$$\frac{\partial}{\partial A_n} \left[S_E^* - \lambda^2 K_E^* \right] = 0 \tag{26}$$

After simplifying equation (26) we get system of homogeneous eq. as

$$C_{11}A_1 + C_{12}A_2 = 0$$
 and
$$C_{21}A_1 + C_{22}A_2 = 0$$
 (27)

The determinant of the coefficient matrix obtained from equation (27) must be zero in order to produce a non-zero solution (frequency equation).

$$\begin{vmatrix} c_{11} & c_{12} \\ c_{21} & c_{22} \end{vmatrix} = 0$$
(28)

After simplifying above equation we get a quadratic equation in λ . With λ representing frequency modes derived from equation (28), the time period of frequency modes is computed as $k = \frac{2\pi}{\lambda}$.

Result And Discussion

Duralumin, an aluminium alloy, is a visco-elastic material that produces the intended results. The calculations for Duralumin make use of the following parameters:

$$E_{0} = 7.08 \times 10^{10} \ N/M^{2},$$

$$G = 2.632 \times 10^{10} \text{ N/M}^2$$

$$\eta = 14.612 \times 10^5 \text{ N s/M}^2$$
,

$$\rho_0 = 2.8 \times 10^3 \text{ kg/M}^3$$
,

$$v = 0.345$$
 and $h_0 = 0.01 \text{ M}$

- For aspect ratios of 1.5 and 2.5, calculations were carried out for the first two frequency modes for various values of the thermal gradient (α), non-homogeneity(m_2), and taper parameter (β).
- II) The first two modes of the frequency parameter in Tables (1) and (4) increases continuously for both aspect ratios of 1.5 and 2.5 for every fixed value of the thermal gradient (α) while the taper parameter (β) increases from 0.2 to 0.6 and non-homogeneity (m_2) stays constant at $\nu = 0.345$. In every cases, the first two modes of the frequency parameter decrease as the thermal gradient (α) values rise from 0.0 to 0.8.
- III) For any fixed value of non-homogeneity (m_2) in Tables (2) and (5), the first two modes of the frequency parameter increase steadily for both aspect ratios of 1.5 and 2.5 as the values of the thermal gradient (α) and taper parameter (β) rise from 0.2 to 0.8 with ν = 0. In every scenario, the first two modes of the frequency parameter drop as the non-homogeneity (m_2) values rise from 0.0 to 1.0.
- In Table (3) and (6), for each fixed value of taper parameter(β), the first two mode of frequency parameter decrease continuously for both aspect ratio 1.5 and 2.5 as value of the thermal gradient (α) and non-homogeneity(m₂) increase from 0.2 to 0.6 with ν = 0.345. As the values of the taper parameter(β) increases from 0.0 to 1.0, the first two mode of frequency parameter increases for all cases.

Table 1. Frequency of simple supported rectangular plate vs Thermal gradient(α) for Aspect Ratio 1.5

| α | $\beta = 0.2, m_2 = 0, \nu = 0.345$ | | $\beta = 0.4, m_2 = 0, \nu = 0.345$ | | $\beta = 0.6, m_2 = 0,$ $\nu = 0.345$ | |
|---|-------------------------------------|-------------|-------------------------------------|-------------|---------------------------------------|-------------|
| | λ_1 | λ_2 | λ_1 | λ_2 | λ_1 | λ_2 |

| 0 | 57.6608 | 430.5953 | 60.2813 | 448.4819 | 63.0982 | 467.9346 |
|-----|---------|----------|---------|----------|---------|----------|
| 0.2 | 54.9658 | 413.0808 | 57.5806 | 431.0280 | 60.3886 | 450.5353 |
| 0.4 | 52.1281 | 394.7905 | 54.7424 | 412.8375 | 57.5460 | 432.4374 |
| 0.6 | 49.1219 | 375.6113 | 51.7426 | 393.8084 | 54.5479 | 413.5491 |
| 0.8 | 45.9121 | 355.3994 | 48.5489 | 373.8130 | 51.3648 | 393.7572 |

Graphical representation of the table-1:

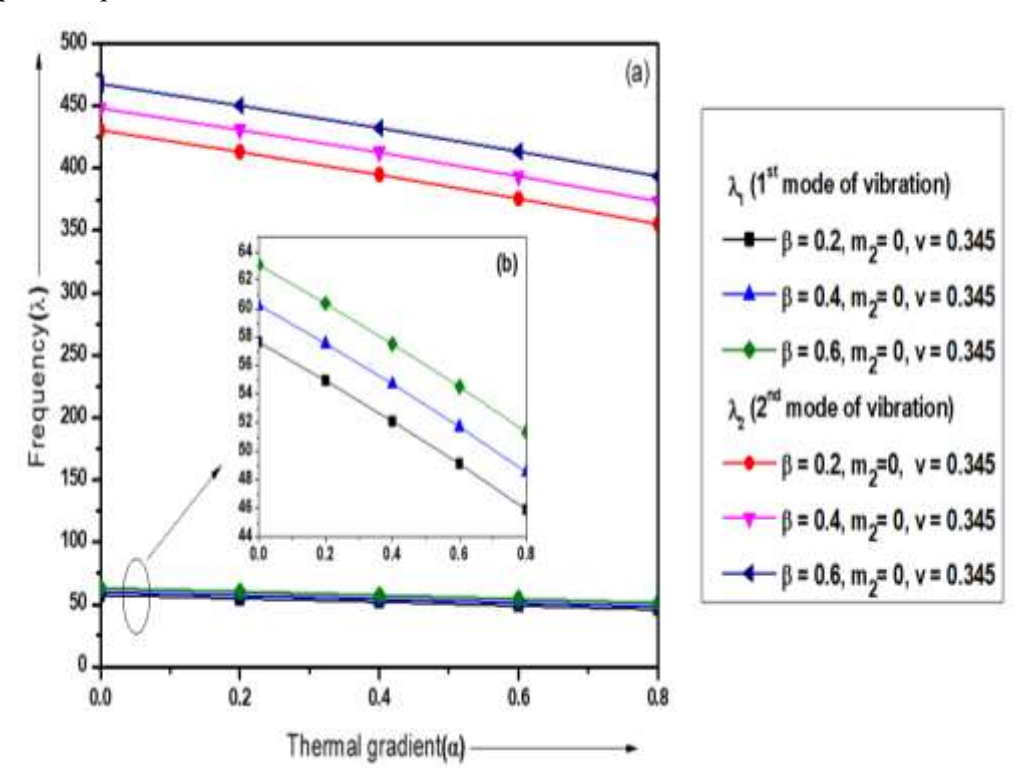


Figure-1: Thermal gradient vs Frequency

Table2. Frequency of simple supported rectangular plate vs Non-Homogeneity(m₂) for Aspect Ratio 1.5

| | $\alpha = \beta = 0.2, \nu = 0$ | | $\alpha = \beta = 0.6, \nu = 0$ | | $\alpha = \beta = 0.8, \nu = 0$ | |
|----------------|---------------------------------|-------------|---------------------------------|-------------|---------------------------------|-------------|
| \mathbf{m}_2 | λ_1 | λ_2 | λ_1 | λ_2 | λ_1 | λ_2 |
| 0.0 | 51.9895 | 388.0317 | 52.7129 | 389.3578 | 53.2293 | 391.3813 |
| 0.2 | 49.5520 | 369.6947 | 50.2089 | 370.4594 | 50.6862 | 372.1593 |
| 0.4 | 47.4281 | 353.7337 | 48.0308 | 354.0710 | 48.4758 | 355.5184 |
| 0.6 | 45.5558 | 339.6762 | 46.1137 | 339.6819 | 46.5315 | 340.9281 |
| 0.8 | 43.8890 | 327.1717 | 44.4092 | 326.9160 | 44.8038 | 327.9989 |
| 1 | 42.3928 | 315.9538 | 42.8807 | 315.4893 | 43.2553 | 316.4377 |

Graphical representation of the table-2:

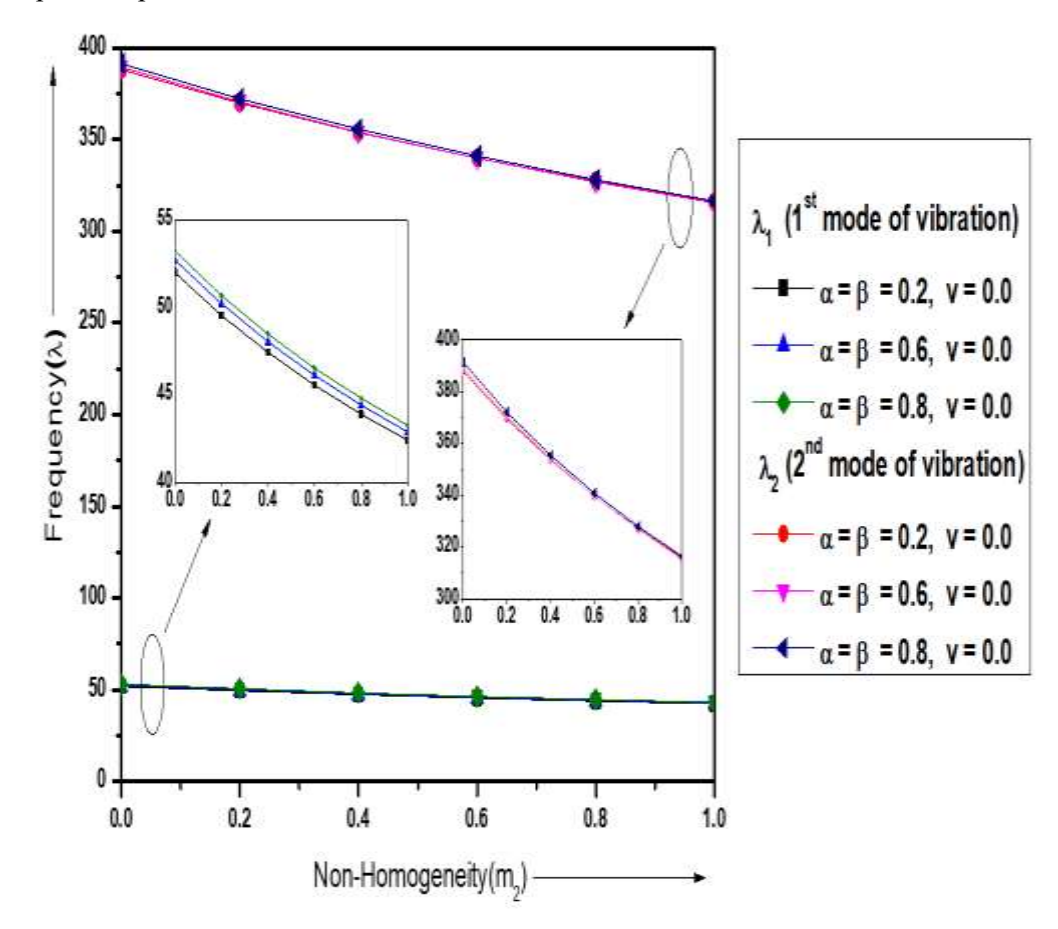


Figure-2: Non-Homogeneity vs Frequency

Table 3. Frequency of simple supported rectangular plate vs Taper constant(β) for Aspect Ratio 1.5

| | $\alpha = m_2 = 0.2, \nu = 0.345$ | | $\alpha = m_2 = 0.4, \nu = 0.345$ | | $\alpha = m_2 = 0.8, \nu = 0.345$ | |
|-----|-----------------------------------|-------------|-----------------------------------|-------------|-----------------------------------|-------------|
| β | λ_1 | λ_2 | λ_1 | λ_2 | λ_1 | λ_2 |
| 0 | 50.1170 | 378.3390 | 45.3905 | 345.4425 | 36.7436 | 286.2095 |
| 0.2 | 52.3888 | 393.5601 | 47.5547 | 359.8946 | 38.7589 | 299.6551 |
| 0.4 | 54.8624 | 410.3737 | 49.9086 | 375.8674 | 40.9417 | 314.4937 |
| 0.6 | 57.5196 | 428.6701 | 52.4343 | 393.2489 | 43.2739 | 330.6070 |
| 0.8 | 60.3422 | 448.3324 | 55.1139 | 411.9211 | 45.7383 | 347.8744 |
| 1 | 63.3130 | 469.2423 | 57.9309 | 431.7667 | 48.3197 | 366.1790 |

Graphical representation of the table-3:

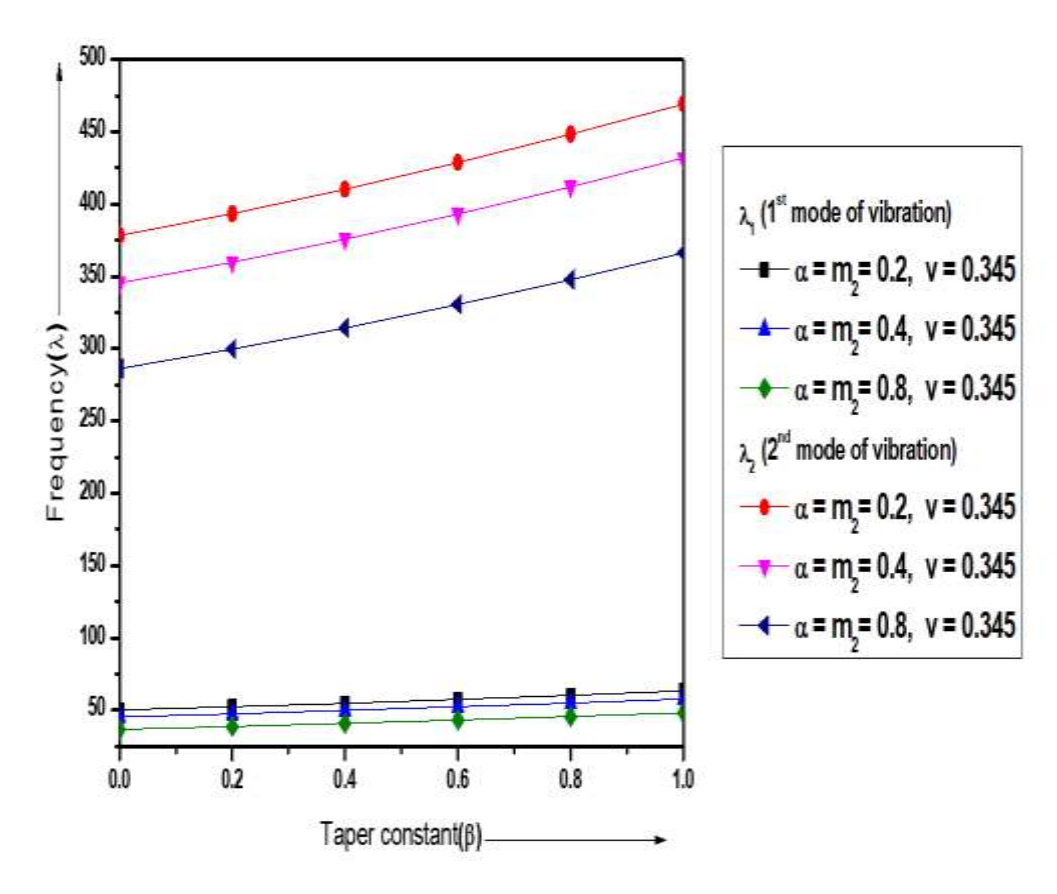


Figure-3: Taper constant vs Frequency

Table 4. Frequency of simple supported rectangular plate vs Thermal gradient(α) for Aspect Ratio 2.5

| | $\beta = 0.2, m_2 = 0, \nu = 0.345$ | | β =0.4, m_2 = 0, ν =0.345 | | β =0.6, m_2 = 0, ν =0.345 | |
|-----|-------------------------------------|-------------|---------------------------------------|-------------|---------------------------------------|-------------|
| α | λ_1 | λ_2 | λ_1 | λ_2 | λ_1 | λ_2 |
| 0 | 46.1175 | 385.4861 | 47.9804 | 397.5019 | 49.9649 | 410.1599 |
| 0.2 | 43.8635 | 369.4820 | 45.7102 | 381.3286 | 47.6766 | 393.8089 |
| 0.4 | 41.4850 | 352.7527 | 43.3186 | 364.4385 | 45.2697 | 376.7493 |
| 0.6 | 38.9587 | 335.1899 | 40.7834 | 346.7271 | 42.7231 | 358.8802 |
| 0.8 | 36.2524 | 316.6550 | 38.0745 | 328.0615 | 40.0087 | 340.0742 |

Graphical representation of the table-4:

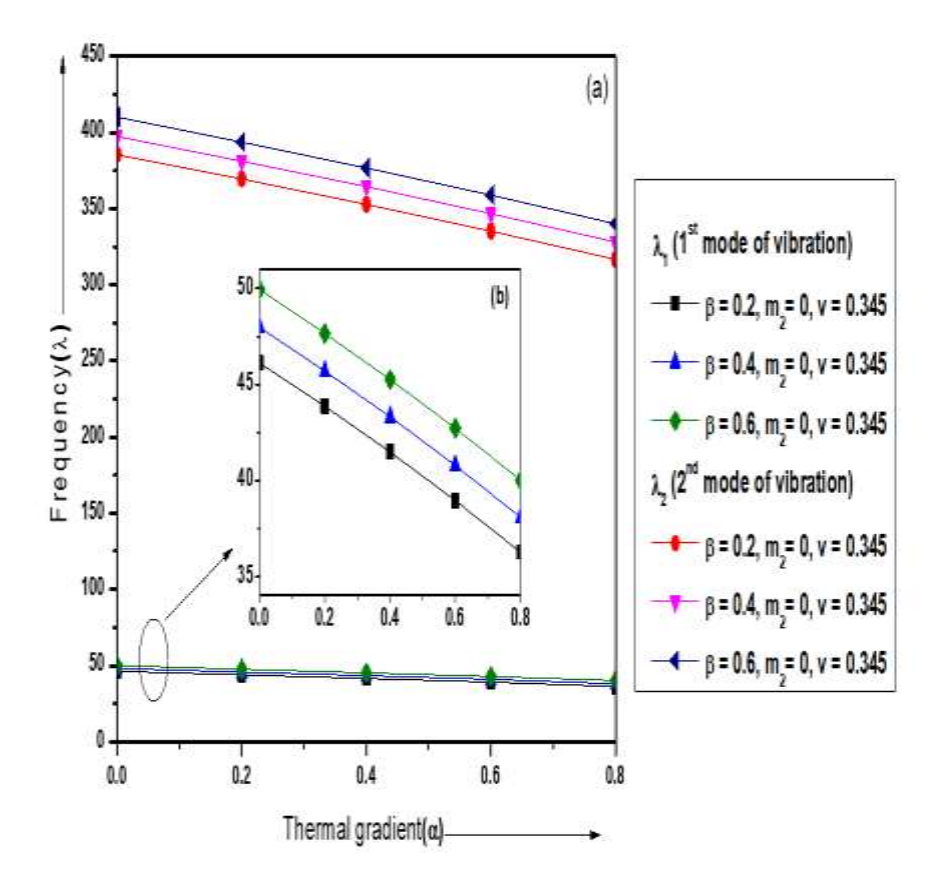


Figure-4: Thermal gradient vs Frequency

Table 5. Frequency of simple supported rectangular plate vs Non-Homogeneity(m_2) for Aspect Ratio 2.5

| | $\alpha = \beta = 0.2, \nu = 0$ | | $\alpha = \beta = 0$ | $\alpha = \beta = 0.6, \nu = 0$ | | $0.8, \nu = 0$ |
|----------------|---------------------------------|-------------|----------------------|---------------------------------|-------------|----------------|
| $\mathbf{m_2}$ | λ_1 | λ_2 | λ_1 | λ_2 | λ_1 | λ_2 |
| 0.0 | 41.3505 | 346.9228 | 40.8019 | 337.3437 | 40.5111 | 331.7484 |
| 0.2 | 39.4118 | 330.5286 | 38.8635 | 320.9718 | 38.5752 | 315.4584 |
| 0.4 | 37.7225 | 316.2587 | 37.1774 | 306.7741 | 36.8926 | 301.3554 |
| 0.6 | 36.2333 | 303.6906 | 35.6934 | 294.3083 | 35.4127 | 288.9900 |
| 0.8 | 34.9076 | 292.5109 | 34.3739 | 283.2486 | 34.0976 | 278.0322 |
| 1 | 33.7176 | 282.4815 | 33.1907 | 273.3490 | 32.9189 | 268.2336 |

Graphical representation of the table-5:

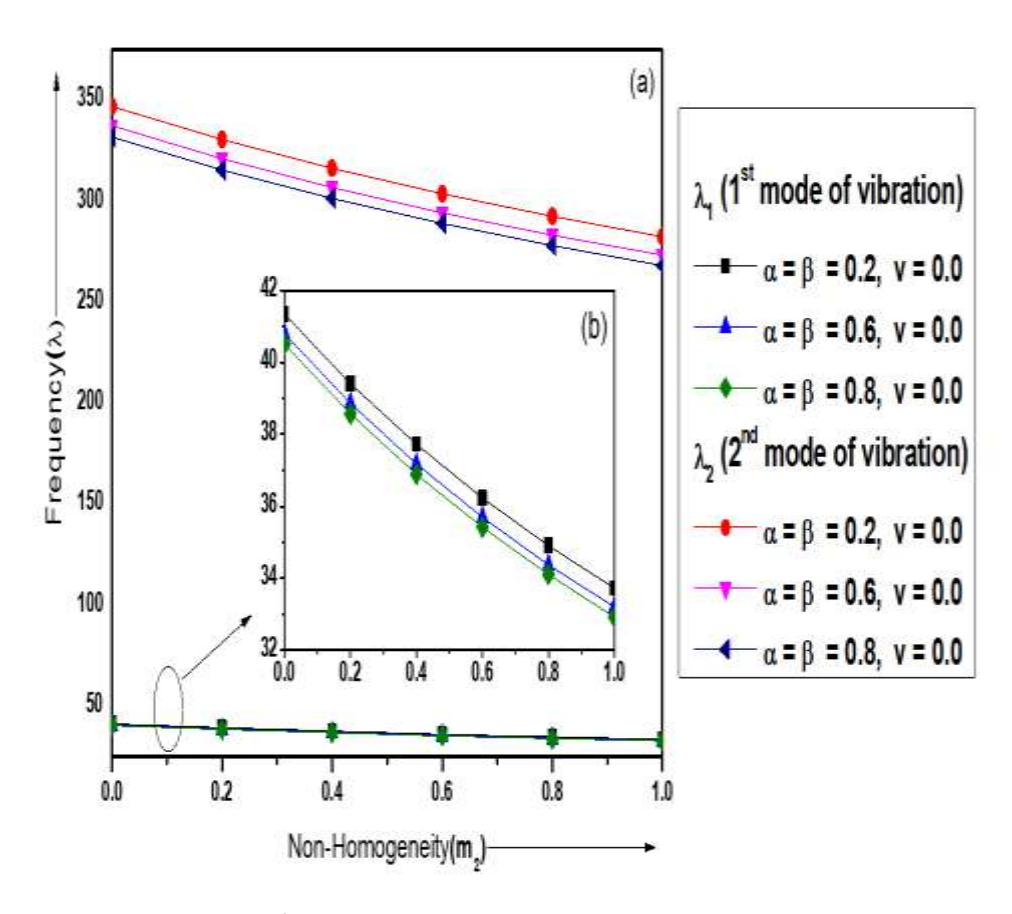


Figure-5: Non-Homogeneity vs Frequency

Table 6. Frequency of simple supported rectangular plate vs Taper constant(β) for Aspect Ratio 2.5

| β | $\alpha = m_2 = 0.2, \nu = 0.345$ | | $\alpha = m_2 = 0.4, \nu = 0.345$ | | $\alpha = m_2 = 0.8, \nu = 0.345$ | |
|-----|-----------------------------------|-------------|-----------------------------------|-------------|-----------------------------------|-------------|
| | λ_1 | λ_2 | λ_1 | λ_2 | λ_1 | λ_2 |
| 0.0 | 40.1848 | 341.6386 | 36.3133 | 311.9610 | 29.2029 | 258.5319 |
| 0.2 | 41.8070 | 352.0218 | 37.8453 | 321.5730 | 30.6041 | 266.9886 |
| 0.4 | 43.5523 | 363.0564 | 39.4934 | 331.8040 | 32.1082 | 276.0051 |
| 0.6 | 45.4114 | 374.6983 | 41.2481 | 342.6104 | 33.7059 | 285.5391 |
| 0.8 | 47.3746 | 386.9037 | 43.1001 | 353.9494 | 35.3877 | 295.5494 |
| 1 | 49.4325 | 399.6306 | 45.0401 | 365.7798 | 37.1448 | 305.9970 |

Graphical representation of the table-6:

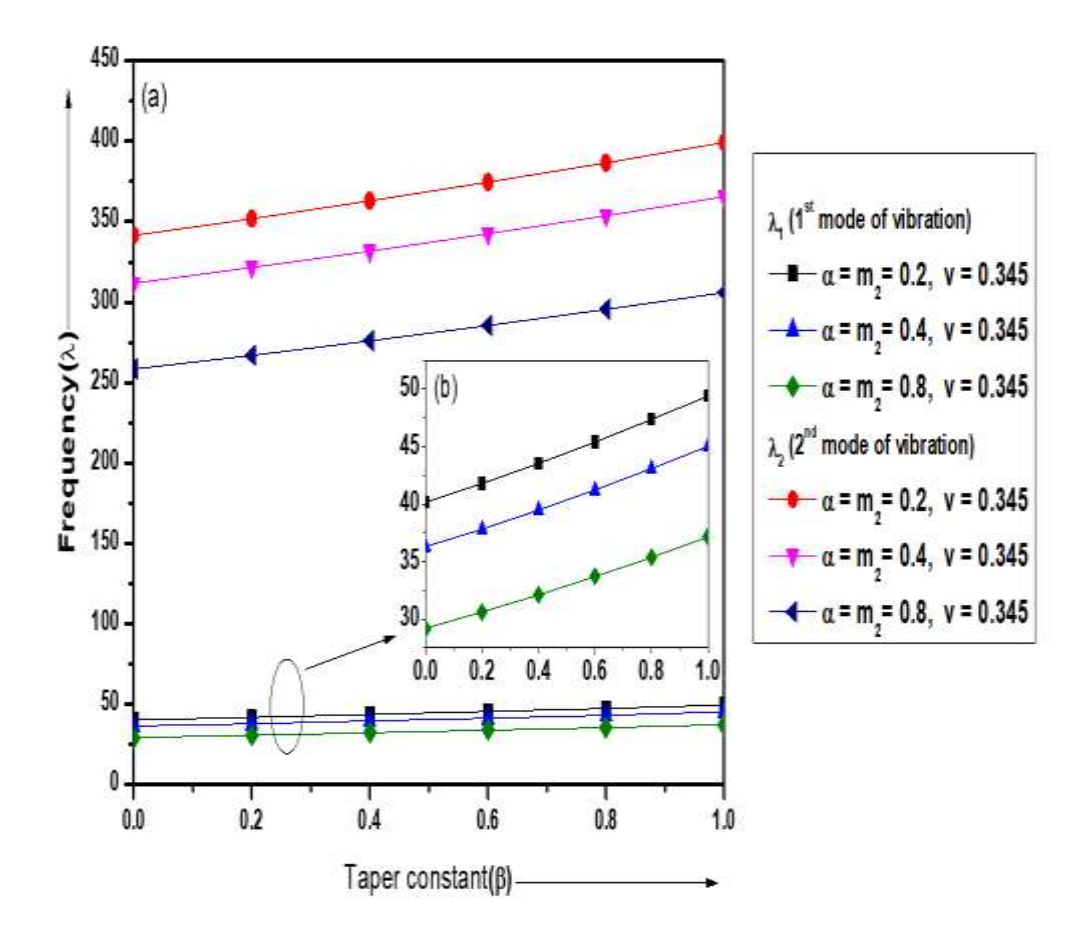


Figure-6: Taper constant vs Frequency

Conclusion

This study investigated the frequencies of isotropic rectangular plates with circular thickness and variations in density and linear temperature. The above result indicates that when the tapering constant (β) increases, the frequency λ_1 and λ_2 decreases at varying values of the temperature gradient (α) and non-homogeneity (m_2). However, an increase in temperature gradient (α) and non-homogeneity (m_2) leads to an increase in frequency. The implementation of circular variation causes the frequency modes λ_1 and λ_2 to vary very slowly, whether they are growing or decreasing. There is no significant increase or decrease in the frequencies.

References

- [1] Sharma, A., Sharma, A.K., Raghav, A.K. and Kumar, V., 2016. Effect of vibration on orthotropic visco-elastic rectangular plate with two dimensional temperature and thickness variation. Indian Journal of Science and Technology, 9(2), p.7. DOI: 10.17485/ijst/2016/v9i2/51314
- [2] Gupta, A.K. and Singhal, P., 2010. Thermal effect on free vibration of non-homogeneous orthotropic visco-elastic rectangular plate of parabolically varying thickness. Applied Mathematics, 1(06), p.456. DOI: 10.4236/am.2010.16060

- [3] Dong, Y.H. and Li, Y.H., 2017. A unified nonlinear analytical solution of bending, buckling and vibration for the temperature-dependent FG rectangular plates subjected to thermal load. Composite Structures, 159, pp.689-701. DOI: 10.1016/j.compstruct.2016.10.001
- [4] Sharma, A., 2019. Vibration frequencies of a rectangular plate with linear variation in thickness and circular variation in Poisson's ratio. Journal of Theoretical and Applied Mechanics, 57(3), pp.605-615. DOI: 10.15632/jtam-pl/109707
- [5] Khanna, A. and Kaur, N., 2014. Vibration of non-homogeneous plate subject to thermal gradient. Journal of Low Frequency Noise, Vibration and Active Control, 33(1), pp.13-26. DOI:10.1260/0263-0923.33.1.13
- [6] Panda, S.K. and Ramachandra, L.S., 2010. Buckling of rectangular plates with various boundary conditions loaded by non-uniform inplane loads. International Journal of Mechanical Sciences, 52(6), pp.819-828. DOI: 10.1016/j.ijmecsci.2010.01.009
- [7] Tang, Y. and Wang, X., 2011. Buckling of symmetrically laminated rectangular plates under parabolic edge compressions. International Journal of Mechanical Sciences, 53(2), pp.91-97. DOI: 10.1016/j.ijmecsci.2010.11.005
- [8] Sharma, A., 2018. Vibrational frequencies of parallelogram plate with circular variations in thickness. In Soft Computing: Theories and Applications: Proceedings of SoCTA 2016, Volume 1 (pp. 317-326). Springer Singapore. DOI: 10.1007/978-981-10-5687-1_29
- [9] Gupta, A., Jain, N.K., Salhotra, R. and Joshi, P.V., 2018. Effect of crack location on vibration analysis of partially cracked isotropic and FGM micro-plate with non-uniform thickness: an analytical approach. International Journal of Mechanical Sciences, 145, pp.410-429. DOI: 10.1016/j.ijmecsci.2018.07.015
- [10] Lal, R. and Saini, R., 2015. Buckling and vibration analysis of non-homogeneous rectangular Kirchhoff plates resting on two-parameter foundation. Meccanica, 50, pp.893-913. DOI: 10.1007/s11012-014-0073-0
- [11] Bhardwaj, R., Mani, N. and Sharma, A., 2021. Time period of transverse vibration of skew plate with parabolic temperature variation. Journal of Vibration and Control, 27(3-4), pp.323-331. DOI: 10.1177/1077546320926887
- [12] Lal, R. and Saini, R., 2017. Mode shapes and frequencies of thin rectangular plates with arbitrarily varying non-homogeneity along two concurrent edges. Journal of Vibration and Control, 23(17), pp.2841-2865. DOI: 10.1177/1077546315623710
- [13] Kumar, A., Lather, N. and Sharma, A., 2019, August. Analysis of time period of isotropic square plate on clamped and simply supported conditions. In AIP Conference Proceedings (Vol. 2142, No. 1). AIP Publishing. DOI: 10.1063/1.5122486
- [14] Sharma, A. and Kumar, P., 2018. Natural Vibration of Square Plate. Soft Computing: Theories and Applications: Proceedings of SoCTA 2017, 742, p.311. DOI: 10.1007/978-981-13-0589-4 29
- [15] Sharma, A. and Kumar, P., 2019. Natural vibration of square plate with circular variation in thickness. In Soft Computing: Theories and Applications: Proceedings of SoCTA 2017 (pp. 311-319). Springer Singapore. DOI: 10.1007/978-981-13-0589-4_29
- [16] Khanna, A. and Singhal, A., 2016. Effect of plate's parameters on vibration of isotropic tapered rectangular plate with different boundary conditions. Journal of Low Frequency Noise, Vibration and Active Control, 35(2), pp.139-151. DOI: 10.1177/0263092316644134
- [17] Gupta, A.K. and Khanna, A., 2007. Vibration of visco-elastic rectangular plate with linearly thickness variations in both directions. Journal of Sound and Vibration, 301(3-5), pp.450-457. DOI: 10.1016/j.jsv.2006.01.074

- [18] Kumar, A., Lather, N., Bhardwaj, R., Mani, N. and Sharma, A., 2018. Effect of linear variation in density and circular variation in Poisson's ratio on time period of vibration of rectangular plate. Vibroengineering Procedia, 21, pp.14-19. DOI: 10.21595/vp.2018.20367
- [19] Kaur, N., Singhal, A. and Khanna, A., 2018. A study on vibration of tapered non-homogeneous rectangular plate with structural parameters. International Journal of Applied Mechanics and Engineering, 23(4), pp.873-884. DOI:10.2478/ijame-2018-0048
- [20] Khanna, A. and Kaur, N., 2016. Effect of thermal gradient on vibration of non-uniform visco-elastic rectangular plate. Journal of The Institution of Engineers (India): Series C, 97, pp.141-148. DOI: 10.1007/s40032-015-0212-y